PID-State Torque Control in Electromechanical Drive Systems Under Stochastic Load

Constantinos Sourkounis, *Member, IEEE*

***Abstract*—Many technical processes with stochastic workflow are characterized by high load peaks. Those load peaks propagate in the power train of the electromechanical drive system to the feeding power grid and at the same time stimulate torsion oscillations. For smoothing the load peaks as well as damping the torque oscillations, a novel torque control was designed. The concept consists of a PID-state control and was compared to standard control methods such as standard PID control. The PID-state control shows distinctive advantages with respect to the reference-variable response and the manipulated variable requirement.**

***Index Terms*—Active damping of torque oscillations, PID state control, pole placement method, torque control.**

I. Introduction

NUMEROUS technical processes feature a stochastic time flow. Characteristic examples of stochastic processes are, for instance, shredder processes and wind energy conversion systems. During execution of these processes, the power train which provides the process with the necessary mechanical power experiences corresponding stochastic load. This is in most of the cases an electromechanical power train. The loads resulting from the process cause corresponding torque peaks in the power train. They propagate through the power train up to the electrical supply grid, where they lead to current peaks as a consequence. Furthermore, torsional vibrations are excited by load peaks which impose additional loads on the power train [1], [2], [14].

In addition to premature material fatigue of the mechanical drive components, they also entail continuous thermal overloading of the asynchronous machine. In addition, they result in peak loads in the power supply net so that the operating costs (demand rate) are increased.

Thus, the derived demands on the electromechanical drive system can be formulated on the basis of long operating life, high availability, and a high utility factor—also with respect to the economical efficiency of the system.

Manuscript received December 19, 2010; revised June 3, 2011; accepted September 1, 2011. Date of publication November 11, 2011; date of current version January 20, 2012. Paper 2010-IACC-509.R1, presented at the 2010 Industry Applications Society Annual Meeting, Houston, TX, October 3–7, and approved for publication in the IEEE Transactions on Industry Applications by the Industrial Automation and Control Committee of the IEEE Industry Applications Society.

The author is with the Research Group for Power Systems Technology, Faculty of Electrical Engineering and Information Science, Ruhr-University Bochum, 44801 Bochum, Germany (e-mail: sourkounis@eele.rub.de).

Color versions of one or more of the figures in this paper are available online at http://ieeexplore.ieee.org.

Digital Object Identifier 10.1109/TIA.2011.2175878

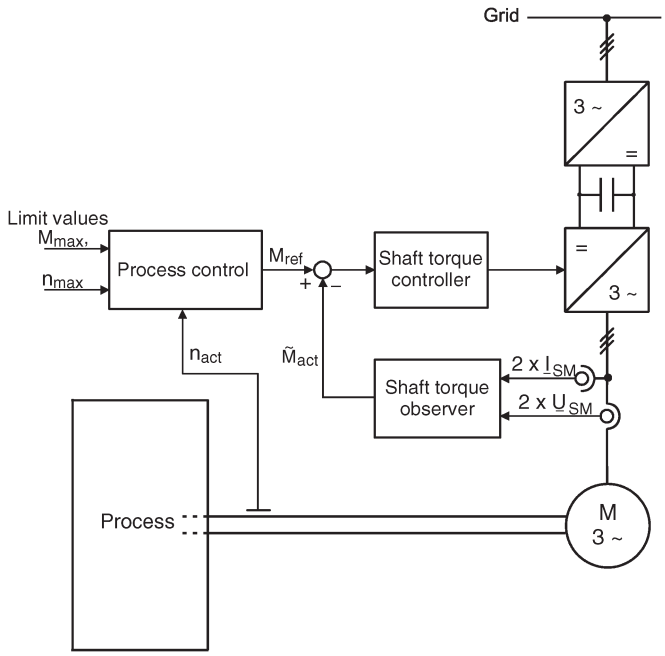

Fig. 1. Basic structure of a drive train system for shredder plants.

II. Dynamic Behavior of the Basic Structure of the Power Train

The basic structure of the control system can be laid out in accordance with the given requirements for the drive system. Essential demands on high availability and by this also long operating life as well as low mains pollution can only be met by minimization of cumulated loads in the electromechanical power train. This minimization of cumulated loads can be realized by two measures. On the one hand, by active damping of the torsional vibrations and on the other by smoothing, the load peaks in the power train. Both measures require a power train structure which allows a dynamic torque control. In addition a "speed-variable operation" is necessary for smoothing the load peaks and thus to avoid the resultant cumulated loads so that the fly-wheel storage effect can be used.

The basic structure of the power train is shown in Fig. 1. The necessary mechanical power for the process is provided by a converter-fed asynchronous machine. The frequency converter offers a dynamic torque impression in the drive train, so that an on-demand power supply can be realized for the process; this is possible by the so-called "internal control" of the converter. Furthermore, on the basis of a suitable concept of shaft torque control, an active torsional vibration damping is aimed for. This means that the shaft torque control has to be planned and

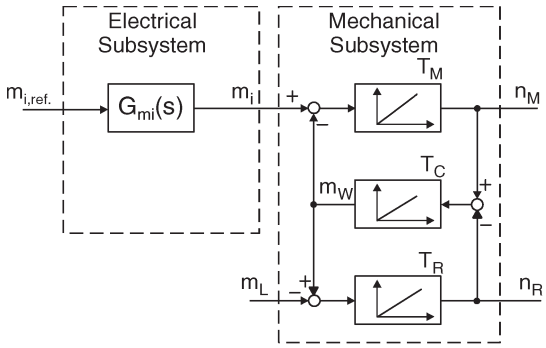

Fig. 2. Simplified mathematical electric-mechanical power train model.

designed to feature a good reference and disturbance response as well. The reference value of the shaft torque control is calculated by a superimposed control structure (process or operating control) according to the requirements.

The basic structure of the power train has been taken as basis for the conceptional design and layout of the torque control. As shown in Fig. 2, it can be divided into a mechanical and electrical subsystem. Based on the general differential equations of movement, the dynamic behavior of the mechanical subsystem is represented by the mathematical model of a two-mass-spring system (see Fig. 2), simplified by the assumption that the mass of the shaft is negligibly low

$$\begin{aligned} \mathrm{M_{mi}} - \mathrm{M_W} &= \mathrm{J_M}\frac{\mathrm{d}\omega_\mathrm{M}}{\mathrm{dt}} \\ \mathrm{M_W} &= \mathrm{C}(\varphi_\mathrm{M} - \varphi_\mathrm{R}) = \mathrm{C}\int(\omega_\mathrm{M} - \omega_\mathrm{R})\mathrm{dt} \\ \mathrm{M_W} - \mathrm{M_L} &= \mathrm{J_R}\frac{\mathrm{d}\omega_\mathrm{R}}{\mathrm{dt}}. \end{aligned} \tag{1}$$

This simplification also means that the mechanical subsystem of the power train and particularly its operating behavior can be defined considerably by only a dominant self-motion [2].

The simplified mathematic model in state space representation can be described as an equation system on the basis of generator speed $\mathrm{n_M}$, load rotor speed $\mathrm{n_R}$, and shaft torque $\mathrm{m_W}$ as state variables, as well as by the input variables air-gap torque $\mathrm{m_i}$ and load torque $\mathrm{m_L}$

$$\begin{bmatrix} \dot{\mathrm{n}}_\mathrm{M} \\ \dot{\mathrm{m}}_\mathrm{W} \\ \dot{\mathrm{n}}_\mathrm{R} \end{bmatrix} = \begin{bmatrix} 0 & -\frac{1}{\mathrm{T_M}} & 0 \\ \frac{\mathrm{T_M}}{(1+\mathrm{v})\mathrm{T_{ef}^2}} & 0 & -\frac{\mathrm{T_M}}{(1+\mathrm{v})\mathrm{T_{ef}^2}} \\ 0 & \frac{1}{\mathrm{T_R}} & 0 \end{bmatrix} \cdot \begin{bmatrix} \mathrm{n_M} \\ \mathrm{m_W} \\ \mathrm{n_R} \end{bmatrix} + \begin{bmatrix} \frac{1}{\mathrm{T_M}} & 0 \\ 0 & 0 \\ 0 & -\frac{1}{\mathrm{T_R}} \end{bmatrix} \cdot \begin{bmatrix} \mathrm{m_i} \\ \mathrm{m_L} \end{bmatrix}. \tag{2}$$

With the starting time constant $\mathrm{T_M}$ of the motor

$$\mathrm{T_M} = \frac{2\pi \mathrm{n_{nom}}}{\mathrm{M_{nom}}}\mathrm{J_M} \tag{3}$$

the starting time constant $\mathrm{T_R}$ of the load rotor mass

$$\mathrm{T_R} = \frac{2\pi \mathrm{n_{nom}}}{\mathrm{M_{nom}}}\mathrm{J_R} \tag{4}$$

the mass inertia ratio v

$$\mathrm{v} = \frac{\mathrm{J_M}}{\mathrm{J_R}} = \frac{\mathrm{T_M}}{\mathrm{T_R}} \tag{5}$$

and the time constant $\mathrm{T_C}$ for the spring constant C applies with

$$\mathrm{T_C} = \frac{\mathrm{M_{nom}}}{2\pi \mathrm{n_{nom}}} \cdot \frac{1}{\mathrm{C}} \tag{6}$$

for the natural angular frequency ω_ef of the mechanical subsystem and its relevant time constant $\mathrm{T_{ef}}$, respectively, [2], [3]

$$\omega_\mathrm{ef} = \frac{1}{\mathrm{T_{ef}}} = \sqrt{\mathrm{C}\left(\frac{1}{\mathrm{J_M}} + \frac{1}{\mathrm{J_R}}\right)}, \quad \mathrm{T_{ef}} = \frac{1}{\omega_\mathrm{ef}} = \sqrt{\frac{\mathrm{T_C T_M}}{(1+\mathrm{v})}}. \tag{7}$$

From the simplified mathematical model, the transfer function of the shaft torque $\mathrm{m_w}$ is derived. After application of the Laplace transformation and scaling, the following transfer function is derived:

$$\mathrm{m_w(s)} = \frac{1}{\mathrm{v}+1} \cdot \frac{1}{\mathrm{s^2 T_{ef}^2}+1} \cdot \mathrm{m_i(s)} + \underbrace{\frac{\mathrm{v}}{\mathrm{v}+1} \cdot \frac{1}{\mathrm{s^2 T_{ef}^2}+1} \cdot \mathrm{m_L(s)}}_{\mathrm{m_L^*}} \tag{8}$$

with $\mathrm{T_{ef}} = (1/\omega_\mathrm{ef}) = \sqrt{\mathrm{T_C T_M}/(1+\mathrm{v})}$, $\mathrm{v} = (\mathrm{J_M}/\mathrm{J_R}) = (\mathrm{T_M}/\mathrm{T_R})$.

Input variables are here the air-gap moment $\mathrm{m_i}$ and the load torque $\mathrm{m_L}$. The mechanical values (mass inertia and spring constant) have been taken into account by introducing the time constants [(3), (4), and (6)].

From the transfer function, a direct correlation occurs between peak load propagation in the power train and the mass inertia ratio v. At increasing mass inertia ratio v at a constant total mass inertia, higher torque peaks have to be expected in the time behavior of the shaft torque.

The electrical subsystem which belongs to the basic structure of the power train consists of the electrical part of the electromechanical power converter (motor, generator, respectively), the electrical grid, and the frequency converter with internal current control [14].

In the nominal speed range (flux is constant), the operating behavior of the electrical subsystem is described by the transfer function (reference-variable response) of the control circuit for the torque-forming current components and by the air-gap moment $\mathrm{M_i}$. It can generally be approximated by a first-order lag element ($\mathrm{PT_1}$) [3]. The substitute time constant $\mathrm{T_{Str}}$ of the approached transfer function for the electrical subsystem corresponds to the control rise time of the control circuit of the torque-forming current components.

A tailored adjustment of the air-gap moment can be realized by superposition of a shaft torque control. The structure of the torque control has to allow a dynamic behavior, so that—in addition to minimization of load peaks—an active damping of the occurred excited torsion vibrations can also be realized.

Since the manipulated value requirements are directly coupled with higher technical complexity, effort is made to achieve a reduction of the manipulated value requirements in addition to the high control dynamics [4].

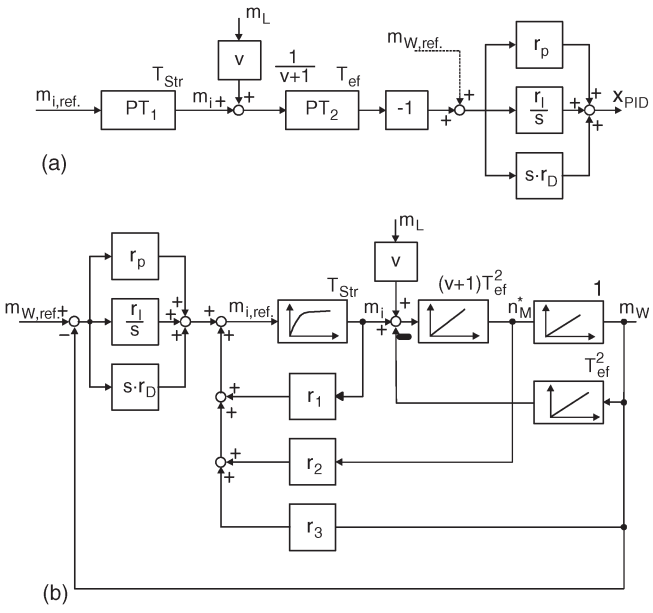

Fig. 3. (a) Block diagram of an expanded controlled system. (b) Block diagram of the PID-state control using the example of a shredder power train.

III. Control Structure and Controller Layout

Based on the general control objectives, the demands on the control circuit for an optimization in the frequency domain can be formulated as follows. An ideal reference-variable response of the control circuit is then available, when for all circuit frequencies ω, the following applies:

$$|\mathrm{G_w}(\mathrm{j}\omega)| \stackrel{!}{=} 1. \tag{9}$$

By this, a universal approach for optimization according to the absolute optimum method is formulated, which—compared with the symmetrical optimum method—does not place any considerable demands on the structure of the controlled system. The controlled system represents a PT3-transmission behavior. The technical literature [7], [13] recommends a controller with PID transmission behavior for this purpose (see Fig. 5).

In consideration of the mentioned requirements a PID-state control has been developed on the basis of a single-loop PID control, and comparing examinations have been carried out. For the design of the PID-state control, the "direct pole placement" method was used [3]–[5], [7], [8].

For a systematic and specific realization of the given demands on the power train by the torque control, the state control basically proves to be of advantage [4].

Since the process quality is directly dependent of the speed in case of the processes discussed, the torque control shall not have any influence on the speed. This means that speed changes have to be disregarded by the torque control (state control). Therefore, the feedback factors for two state values, the motor speed $\mathrm{n_M}$ and the speed of the load mass $\mathrm{n_R}$, shall be set to zero in the ideal case.

For the layout of the state control, the mathematical model of the controlled system, consisting of electrical and mechanical subsystems, is taken as a basis for the general state space diagram. Furthermore, the controlled system has been expanded by the structure of a PID controller [see Fig. 3(a)]. The mathematical model of the expanded control path features is as follows:

$$\begin{aligned} \dot{\boldsymbol{x}}_{\boldsymbol{e}} &= \boldsymbol{A_e x_e} + \boldsymbol{b_e u_e} \\ \boldsymbol{y_e} &= \boldsymbol{c_e^T u_e} \end{aligned} \tag{10}$$

with

$$\boldsymbol{A_e} = \begin{pmatrix} -\frac{1}{\mathrm{T_{Str}}} & 0 & 0 & 0 \\ \frac{1}{(\mathrm{v}+1)\mathrm{T_{ef}^2}} & 0 & -\frac{1}{\mathrm{T_{ef}^2}} & 0 \\ 0 & 1 & 0 & 0 \\ \frac{\mathrm{r_D}}{(\mathrm{v}+1)\mathrm{T_{ef}^2}} & -\mathrm{r_p} & \frac{\mathrm{r_I T_{ef}^2 - r_D}}{\mathrm{T_{ef}^2}} & 0 \end{pmatrix}$$

$$\boldsymbol{x_e} = \begin{pmatrix} \mathrm{m_i} \\ \mathrm{n_M^*} \\ \mathrm{m_W} \\ \mathrm{x_{PID}} \end{pmatrix} \quad \boldsymbol{u_e} = \begin{pmatrix} \mathrm{m_L} \\ \mathrm{m_{i,soll}} \end{pmatrix}$$

$$\boldsymbol{b_{u,e}} = \begin{pmatrix} \frac{1}{\mathrm{T_{Str}}} \\ 0 \\ 0 \\ 0 \end{pmatrix} \quad \boldsymbol{b_{z,e}} = \begin{pmatrix} 0 \\ \frac{\mathrm{v}}{(\mathrm{v}+1)\mathrm{T_{ef}^2}} \\ 0 \\ 0 \end{pmatrix}$$

$$\boldsymbol{c_e} = \begin{pmatrix} 0 \\ 0 \\ 1 \\ 0 \end{pmatrix} \quad \boldsymbol{y_e} = \mathrm{m_W}.$$

It may be derived from the transfer function given in (1). In doing so, instead of the motor speed $\mathrm{n_M}$, a virtual state variable $\mathrm{n_M^*}$ is obtained which is of no importance for the controller layout. This results from the requirement to set the feedback factors of the state values of the speed to zero.

This extension leads accordingly from a PI state control [4], [7] to a "PID-state control". The I-term shall avoid a permanent control deviation in the case of influences by stationary reference input value and disturbance as well [4], [7]. On the other hand, an increase of the control dynamics shall be obtained by the D-element. By an appropriate placement of the resulting second null, the poles of the closed control circuit can be more easily displaced to higher negative values of the real axis in the case of low feedback factors (Fig. 5).

If the expanded controlled system is closed by state feedback, the state values $\boldsymbol{x_s}$ and $\mathrm{x_{PID}}$ are fed back via the feedback factors $\boldsymbol{r_x}$ and $\mathrm{r_{PID}}$. Since the parameters of the PID expansion still have to be determined, the feedback factor $\mathrm{r_{PID}}$ can arbitrarily be set to one.

Therefore, the following is applicable for the feedback vector $\boldsymbol{r}$:

$$\boldsymbol{r} = \begin{pmatrix} \boldsymbol{r_x} \\ 1 \end{pmatrix} = \begin{pmatrix} \mathrm{r_1} \\ \mathrm{r_2} \\ \mathrm{r_3} \\ 1 \end{pmatrix} \tag{11}$$

and for the control value $\mathrm{u} = \mathrm{m_{i,ref.}}$ the following relation:

$$\mathrm{m_{i,ref.}} = \boldsymbol{r}^{\mathrm{T}} \boldsymbol{x}_{\mathrm{e}} = \begin{pmatrix} \mathrm{r_1} & \mathrm{r_2} & \mathrm{r_3} & 1 \end{pmatrix} \begin{pmatrix} \mathrm{m_i} \\ \mathrm{n_M^*} \\ \mathrm{m_W} \\ \mathrm{x_{PID}} \end{pmatrix}. \tag{12}$$

Based on the assumption, that $\mathrm{w(s)} = \mathrm{m_{W,ref.}(s)} = 0$ and $\mathrm{z(s)} = \mathrm{m_L} = 0$, the homogenous differential state equation of

the state control can be derived from (10) and (12)

$$\dot{\boldsymbol{x}}_{\boldsymbol{e}}(\mathrm{t}) = \boldsymbol{A}_{\boldsymbol{e}}\boldsymbol{x}_{\boldsymbol{e}}(\mathrm{t}) + \boldsymbol{b}_{\boldsymbol{u},\boldsymbol{e}}\boldsymbol{r}^{\boldsymbol{T}}\boldsymbol{x}_{\boldsymbol{e}}(\mathrm{t}) = (\boldsymbol{A}_{\boldsymbol{e}} + \boldsymbol{b}_{\boldsymbol{u},\boldsymbol{e}}\boldsymbol{r}^{\boldsymbol{T}})\boldsymbol{x}_{\boldsymbol{e}}(\mathrm{t}). \tag{13}$$

For the Laplace range, the following then applies

$$\mathrm{s}\boldsymbol{x}_{\boldsymbol{e}}(\mathrm{s}) - \boldsymbol{x}_{\boldsymbol{e}}(\mathrm{t}_0) = (\boldsymbol{A}_{\boldsymbol{e}} + \boldsymbol{b}_{\boldsymbol{e}}\boldsymbol{r}^{\boldsymbol{T}})\boldsymbol{x}_{\boldsymbol{e}}(\mathrm{s}). \tag{14}$$

The solution of the homogenous differential state equation of the state control has the characteristic equation

$$\det\left[\mathrm{s}\boldsymbol{E} - (\boldsymbol{A}_{\boldsymbol{e}} + \boldsymbol{b}_{\boldsymbol{e}}\boldsymbol{r}^{\boldsymbol{T}})\right] = 0. \tag{15}$$

The Polynomial coefficients are functions of the elements of the feedback vector $\boldsymbol{r}$. By placement of the poles $\mathrm{Sp1}, \ldots, \mathrm{Sp4}$ of the closed control circuit, one obtains the polynomial

$$\mathrm{P(s)} = (\mathrm{s} - \mathrm{s_{p1}})(\mathrm{s} - \mathrm{s_{p2}})(\mathrm{s} - \mathrm{s_{p3}})(\mathrm{s} - \mathrm{s_{p4}}) = 0. \tag{16}$$

By coefficient comparison of both polynomials, the equation system is derived, on the basis of which the feedback factors can be determined.

At first, for the layout of the controller, the position of the poles of the closed control circuit is determined. The eigenvalues of the open loop

$$\boldsymbol{\lambda} = \begin{pmatrix} \lambda_1 \\ \lambda_2 \\ \lambda_3 \\ \lambda_4 \end{pmatrix} = \begin{pmatrix} -\frac{1}{\mathrm{T_{Str}}} \\ \frac{\mathrm{j}}{\mathrm{T_{ef}}} \\ -\frac{\mathrm{j}}{\mathrm{T_{ef}}} \\ 0 \end{pmatrix} \tag{17}$$

shall be displaced by the PID-state control to $\mathrm{Sp1}, \ldots, \mathrm{Sp4}$.

In a first step, the new position of the conjugate complex pair of eigenvalues of the mechanical subsystem $\lambda_{2,3}$ is determined to be $\mathrm{s_{p2,3}}$. The conjugate complex pair of eigenvalues is replaced according to

$$\mathrm{s_{p2,3}} := -\frac{\mathrm{b}}{\mathrm{T_{ef}}} \pm \frac{\mathrm{jb}}{\mathrm{T_{ef}}}. \tag{18}$$

The pair of eigenvalues fulfills a natural damping requirement according to

$$d_{\mathrm{sp2,3}} = -\frac{\mathrm{Re(s_{p2,3})}}{|\mathrm{s_{p2,3}}|} = \frac{1}{\sqrt{2}}. \tag{19}$$

Parameter b determines the distance of the pole pair from the axis origin and thus the dynamics. At a value $\mathrm{b} = 1$, the damping is increased to 0.707 (compared to the uncontrolled system) without changing the natural frequency (see Fig. 4).

In order to maintain the determined dynamics of the pair of eigenvalues on the one hand and keep the manipulated variable demand low on the other, the two remaining eigenvalues of the open control circuit $\lambda_{1,4}$ are replaced by the PID-state control to the value

$$\mathrm{s_{p1,4}} = -\frac{\mathrm{b}\sqrt{2}}{\mathrm{T_{ef}}}. \tag{20}$$

Hereby, the poles of the closed state control circuit are moved along the real axis, so that all poles are positioned on the semicircle of radius

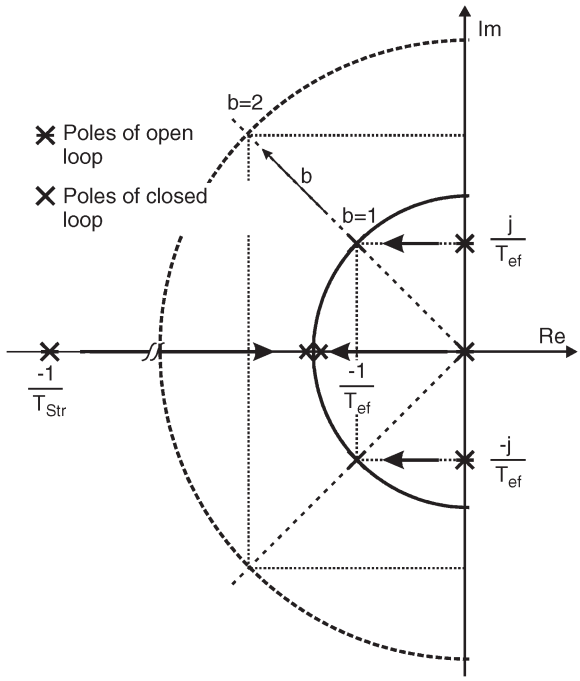

Fig. 4. Position of poles of the open and closed control circuits (PID-state control).

$$R_{sp} = \frac{b\sqrt{2}}{T_{ef}}. \tag{21}$$

By comparison of the coefficients of both polynomials [(22) and (23)], the equation system for determination of the feedback factor $\boldsymbol{r}$ is obtained. Here, the feedback factor $\mathrm{r_2}$ is set to null as a result of the demand that speed changes have to be disregarded by the torque control (state control). The solution of the following equation system:

$$\begin{aligned} \mathrm{r_1} &= \frac{\mathrm{T_{ef}} - 2(\sqrt{2}+1)\mathrm{bT_{Str}}}{\mathrm{T_{ef}}} \\ \mathrm{r_2} &= \mathrm{r_D} - \left(-1 + 4(1+\sqrt{2})\mathrm{b}^2\right)(1+\mathrm{v})\mathrm{T_{Str}} \stackrel{!}{=} 0 \\ \mathrm{r_3} &= \frac{(2+\mathrm{v}-(1+\mathrm{v})\mathrm{r_1})\mathrm{T_{ef}} - 4(1+\sqrt{2})\mathrm{b}^3(1+\mathrm{v})\mathrm{T_{Str}}}{\mathrm{T_{ef}}} \\ \mathrm{r_I} &= \frac{4\mathrm{b}^4(1+\mathrm{v})\mathrm{T_{Str}}}{\mathrm{T_{ef}^2}} \end{aligned} \tag{22}$$

delivers the values of the feedback vector. The feedback factors $\mathrm{r_1}$ and $\mathrm{r_3}$ as well as the parameters of the PID expansion $\mathrm{r_I}$ and $\mathrm{r_D}$ are functions of the parameters of the controlled system and of parameter b

$$\begin{aligned} \mathrm{r_1} &= \frac{\mathrm{T_{ef}} - 2(\sqrt{2}+1)\mathrm{bT_{Str}}}{\mathrm{T_{ef}}}, \\ \mathrm{r_3} &= \frac{\mathrm{T_{ef}} - 2(1+\sqrt{2})\mathrm{b}(-1+2\mathrm{b}^2)(1+\mathrm{v})\mathrm{T_{Str}}}{\mathrm{T_{ef}}} \\ \mathrm{r_I} &= \frac{4\mathrm{b}^4(1+\mathrm{v})\mathrm{T_{Str}}}{\mathrm{T_{ef}}}, \\ \mathrm{r_D} &= \left(-1 + 4(1+\sqrt{2})\mathrm{b}^2\right)(1+\mathrm{v})\mathrm{T_{Str}}, \\ \mathrm{r_2} &= 0, \quad \mathrm{r_p} = 1. \end{aligned} \tag{23}$$

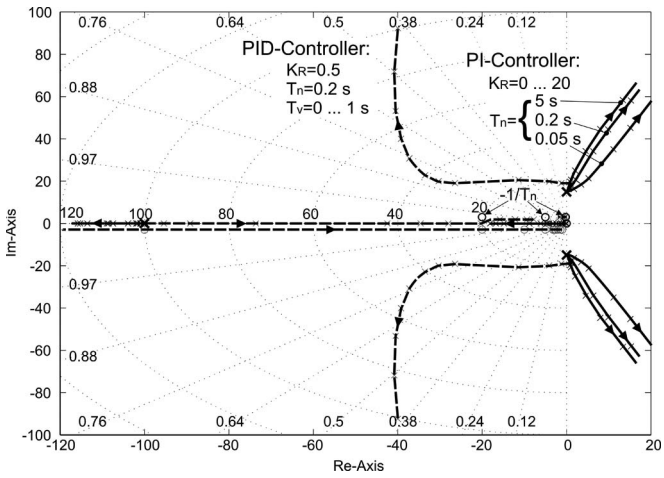

Fig. 5. Comparison of the root locus of a shaft torque control circuit with PI and PID controller; x : pole, o : zero points.

In order to obtain a closed-form solution of the underdetermined equation system, which results by the comparison of the coefficients, the proportional factor r_p of the PID element has been defined. The proportional factor r_p should have a low value to ensure that the required manipulated variable can be kept low [6]. On the other hand, a small proportional factor r_p could possibly lead to lower control dynamics. The control-oriented aspects mentioned made the quantity one to be a reasonable choice.

IV. Simulation Studies of the PID-State Control

The stationary and dynamic behavior of the shaft torque control circuit has been examined by simulation. For basic comparative examinations, the behavior of the observer necessary for estimating the actual shaft torque value has been approached on the basis of a first-order lag element. Since the technical literature [4], [9]–[11], deals in detail with the problems of observers of nonmeasurable actual values and control values, a detailed investigation or layout of an observer has been omitted in this case.

The results of the simulation investigations can be taken from the root locus in Fig. 5 and the time curves of the system quantities in Figs. 6–8. It is evident from Fig. 5 that a sufficient damping cannot be obtained by a PI control in contrast to a PID control.

Therefore, the designed PID-state control has been only examined and compared in detail with single-loop PID control (see Fig. 9). As reference, the uncontrolled drive train system is used. Fig. 6 shows the time curves of the system quantities at an open-loop drive train (compare Fig. 2). Following a jumping alteration of the reference variables, the power train is excited by a pulse-shaped load torque. This excites torsional vibration with an amplitude of up to the 4.5 times the rated torque.

By means of the PID controller, the amplitude of the excited torsional vibration has been reduced to approximately 3% of the rated torque. Less sufficient proved to be the reference-variable response and the manipulated value required. At a

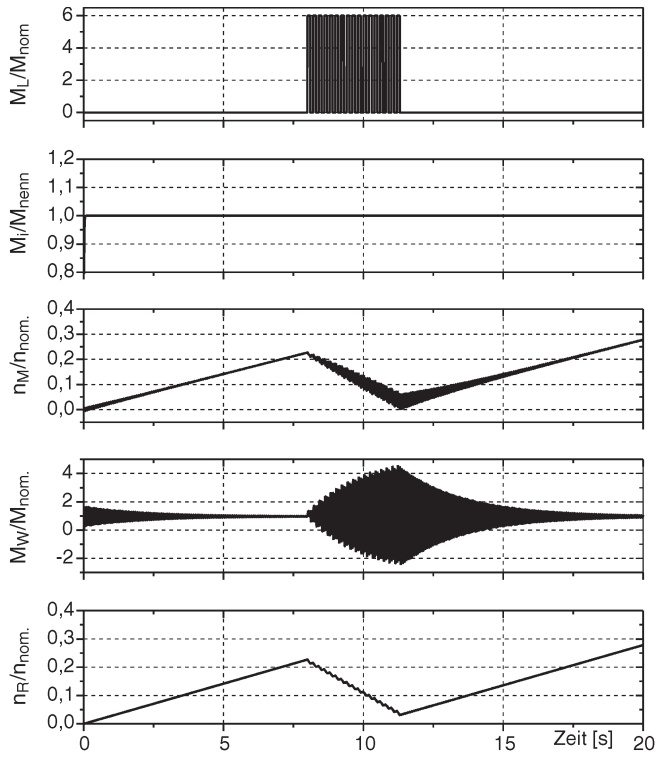

Fig. 6. Time curves of system quantities at uncontrolled power train; impression of a constant electrical moment, air-gap torque, effective passive damping $k_d = 1$ p.u.

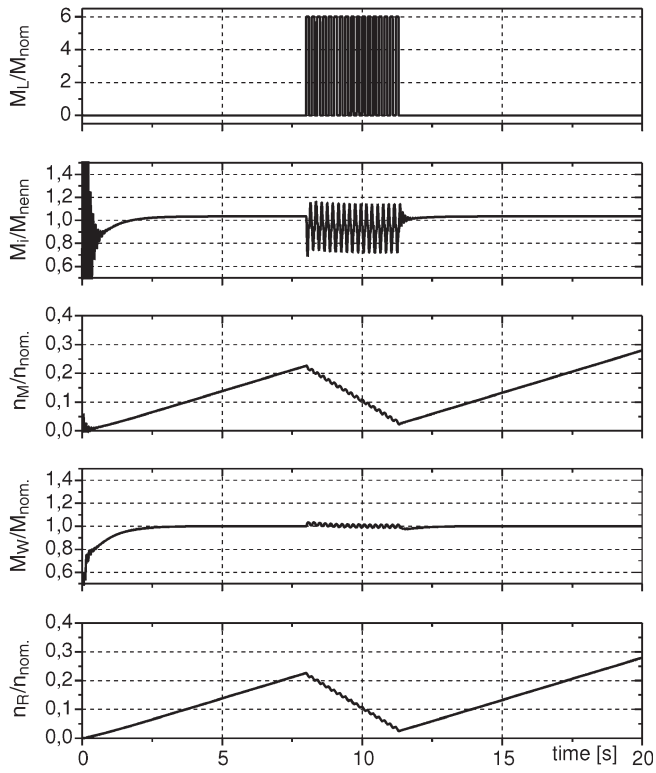

Fig. 7. Time curves of system quantities at PID control of the shaft torque.

manipulated value of 2.8 times the rated torque, a control rise time of approximately 120 ms has been reached.

By variation of parameter b, an optimum could be obtained between control dynamics on the one hand and minimization

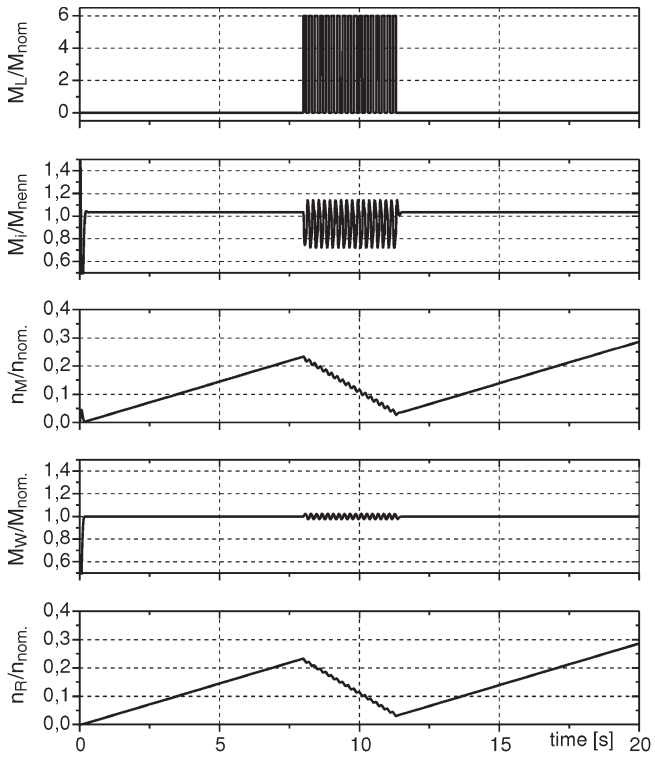

Fig. 8. Simulated time behavior of system variables at PID-state control.

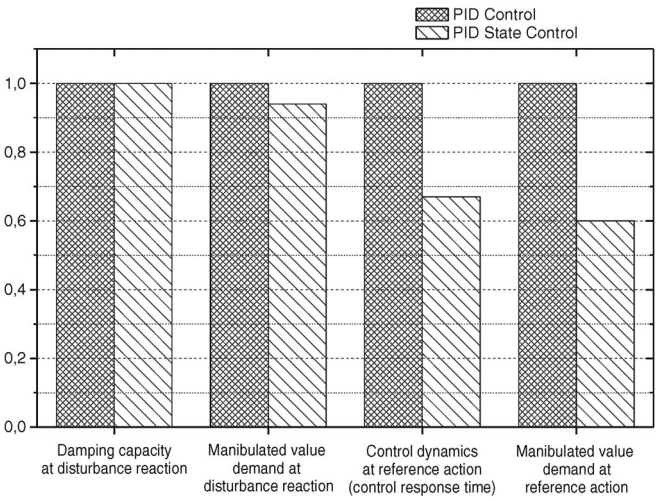

Fig. 9. Comparison of the examined control concepts.

of the required manipulated variable on the other. This is demonstrated in Fig. 8. Here, the time curves of the state values of the control circuit are illustrated. The time curves show a considerable damping of the excited torsional vibrations.

The PID-state control reduces the amplitude of the torsion vibrations to approximately 3% of the rated torque. At the same time, no increase of the average value of the shaft torque is observed. This proves that speed changes do not have any influence on the time curve of the shaft torque. As desired, a complete decoupling of the internal control from the process flow and process control (speed control) is realized.

In contrast to the single-loop PID control, the PID-state control features a lower manipulated variable demand (Figs. 7 and 8). This is obvious in the reference-variable response. At a specific utilization of the manipulated variable range of 1.5 times the rated value, which is in technical view tolerable, a control rise time of 80 ms compared to 120 ms is obtained with the single-loop PID control.

The PID-state control shows distinctive advantages with respect to the reference-variable response. The manipulated variable requirement of the single-loop PID control is higher by a factor 1.65 at lower control dynamics.

V. Experimental Investigation

The results of the analytical and simulation examinations were validated by experimental investigations on a laboratory shredder plant test bench. The setup of the test bench is shown in Fig. 10. The drive train of the test bench has a nominal power of 16 kW and simulates the stationary and dynamical behavior of a real plant with 2.5-MW nominal power.

For the investigations, a PID-state control was compared to a single-loop PID control and the directly grid coupled induction machine as in the original plant.

In the first step, the examination was based on a synthetic load input function. This was derived from the knowledge gained in field tests. The load input function has a pulse shape evoked by the blow of the hammers on the scrap metal. The synthetic load input function can be reproduced easily so that the drives under consideration can be tested at exactly the same rate as the load input function.

In the present application, the time diagram of the drive shaft torque is used for the comparison of different controls. The time diagrams of the drive shaft torque from the experiments (cf. Figs. 11–13) and, likewise, those simulated demonstrate that the drive system of the asynchronous machine with single-loop PID torque control displays meaningful damping of both peak loads and oscillations. Torque peaks in the drive train were reduced to 50% of the nominal value versus 110% in the operation of the existing drive system with directly grid coupling. The amplitude of the load-induced oscillations in the mechanical drive train is diminished by PID control to 40% of the nominal torque by means of the underlying torque control mechanism, compared to 90% in the existing drive system. By the PID-state control, the load peaks show an average value of 25% of the nominal value. The amplitude of the load-induced oscillations in the mechanical drive train is reduced to 18% of the nominal torque.

Furthermore, the drive controls are also tested with the real process load. The load caused by the process was adjusted by the feeding of the scrap material having only an impact on the average load. The resulting time diagram of the load is subject to a stochastic characteristic.

It has been proven to be convenient to use the load spectrum's frequency distribution as a basis for evaluating the drive control, based on the formulated requirements by means of increasing the availability and utilization level and minimizing the load spectrum. There is a direct connection between the frequency distribution of the load spectrum and the reliability as well as the availability.

Fig. 14 shows the load spectrum distribution in the shaft of the drive system with PID-state control compared to drive

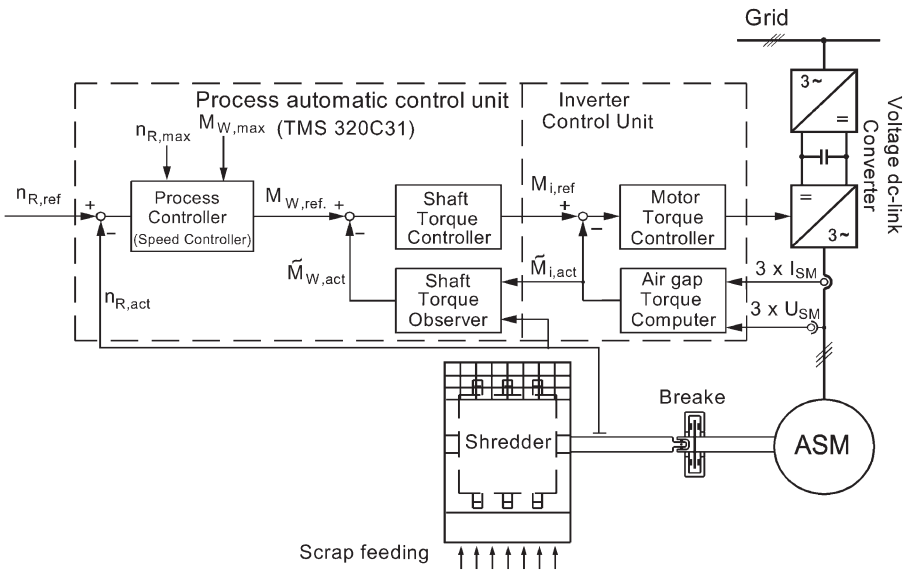

Fig. 10. Basic structure of the laboratory shredder plant test bench.

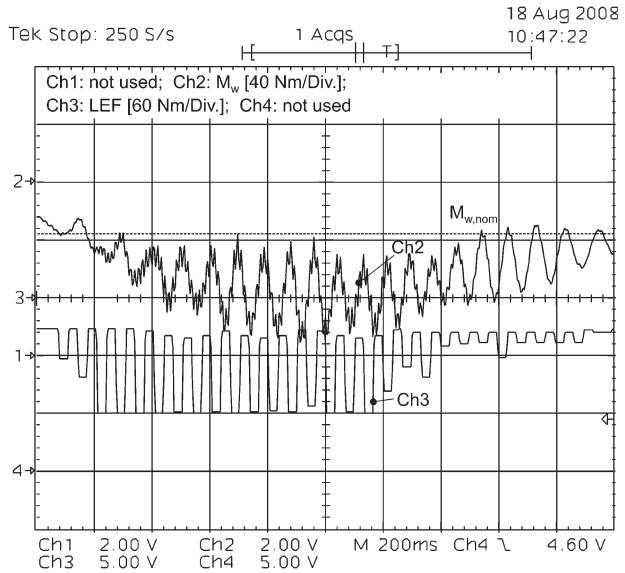

Fig. 11. Record of the shaft torque with synthetic load input function from the drive system with a the directly grid coupled induction machine.

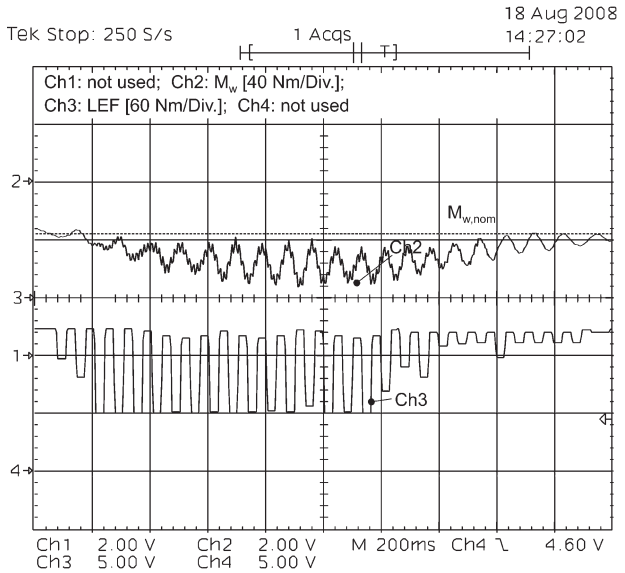

Fig. 12. Record of the shaft torque with synthetic load input function from the drive system with single-loop PID control.

system with single-loop PID control and to the standard drive train. The load peaks could be limited to 1.5 times the rated moment by PID-state control of shaft torque. Overall, there was a distinct shift of the load spectrum distribution toward low amplitudes. The here achieved load spectrum minimization has a qualitative significance regarding the application in commercial shredder plants. This is because of the fact that there is a direct connection between the parameters of the drive train and the dynamics, as well as the demand of manipulated value [1], [14].

The observations made using the example of the shredder operation have the advantage of being transferable to other procedural plants with similar load spectrums.

VI. Conclusion

A new control to minimize the cumulative load in the electromechanical drive of plants with a stochastic process characteristic like shredder plants or wind energy converters has been designed and developed. The control is based on a state control structure, which has been extended by elements with a PID transmission behavior. The I-term avoids a permanent control deviation in the case of influences by both stationary reference input value and disturbance. On the other hand, an increase of the control dynamics is obtained by the D-element. By an appropriate placement of the resulting second null, the poles of the closed control circuit can be more easily displaced to higher negative values of the real axis in the case of low feedback factors.

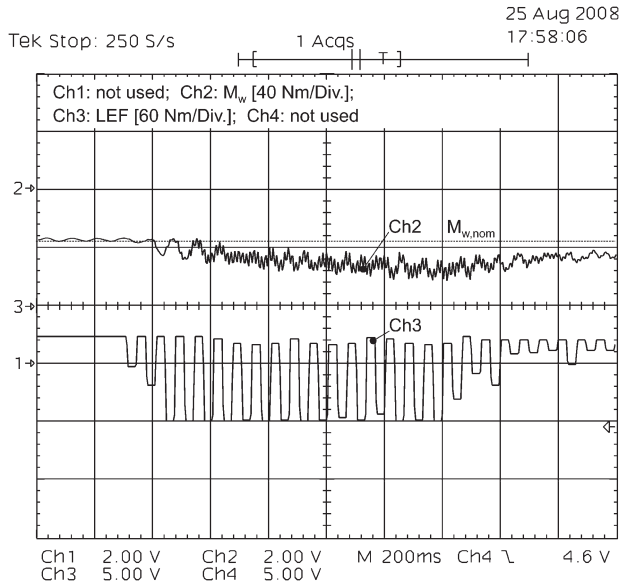

Fig. 13. Record of the shaft torque with synthetic load input function from the drive system with PID-state control.

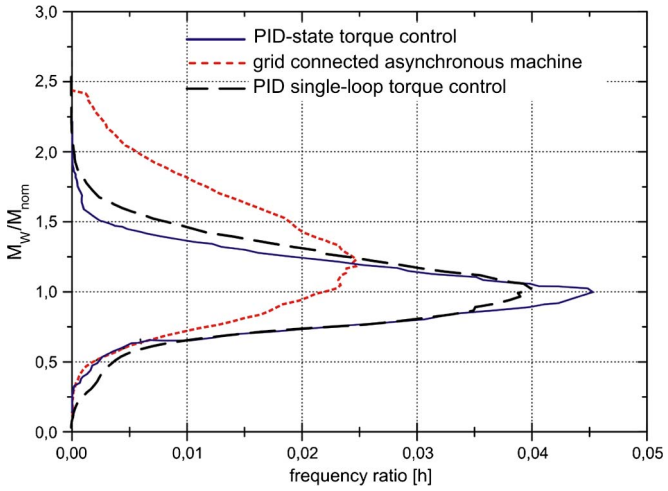

Fig. 14. Frequency distribution of the shaft torque.

For an application on shredder plants the PID-state control has been examined in comparison to single-loop PID control by simulations and experimental studies on a shredder test bench. The results show distinctive advantages with respect to the reference-variable response dynamics and the load spectrum minimization in the power train with a low effort on manipulated values.

REFERENCES

[1] C. Sourkounis, "S-curve-control for active load peak damping in the drive train," in *Proc. IEEE 6th Int. Conf. Workshop CPE*, Badajoz, Spain, May 20–22, 2009, pp. 337–342.

[2] C. Sourkounis, "Drehzahlelastische Antriebe unter stochastischer Belastungen (Speed flexible power drivers under stochastic load)," Habilitationsschrift, TU Clausthal, Clausthal-Zellerfeld, Germany, 2004.

[3] M. Krüger, "Eine anwendungsorientierte Methode zum Entwurf von Zustandsregelungen für elektro-mechanische Hochleistungs-Antriebssysteme," Ph.D. dissertation, TU Clausthal, Clausthal-Zellerfeld, Germany, 1994.

[4] M. Goslar, "Ein Beitrag zur anwendungsorientierten Zustandsregelung elektrischer Hochleistungsantriebe," Ph.D. dissertation, TU Clausthal, Clausthal-Zellerfeld, Germany, 1998.

[5] J. Lunze, *Regelungstechnik 1; 3. Auflage*. Berlin, Germany: Springer-Verlag, 2001.

[6] U. Konigorski, "Entwurf strukturbeschränkter Zustandsregelungen unter besonderer Berücksichtigung des Störverhaltens," *Automatisierungstechnik*, vol. 35, pp. 457–463, 1987.

[7] L. Wendt, *Taschenbuch der Regelungstechnik*. Thun und Frankfurt am Main, Germany: Verlag Harri Deutsch, 1998.

[8] J.-H. Kim and K.-K. Choi, "Design of direct pole placement PID self-tuners," *IEEE Trans. Ind. Electron.*, vol. IE-34, no. 3, pp. 351–356, Aug. 1987.

[9] S. Takagi and N. Uchiyama, "Robust control system design for SCARA robots using adaptive pole placement," *IEEE Trans. Ind. Electron.*, vol. 52, no. 3, pp. 915–921, Jun. 2005.

[10] D. G. Luenberger, "Observing the state of a linear system," *IEEE Trans. Mil. Electron.*, vol. MIL-8, no. 2, pp. 74–80, Apr. 1964.

[11] D. G. Luenberger, "An introduction to observers," *IEEE Trans. Autom. Control*, vol. AC-16, no. 6, pp. 596–602, Dec. 1971.

[12] C. Sourkounis, "H∞-control algorithm for dynamic damping of torsional vibrations in mechatronical drive systems," in *Proc. 35th IEEE IECON*, Porto, Portugal, 2009, pp. 5567–5573.

[13] A. Buxbaum and K. Schierau, *Berechnung von Regelkreisen der Antriebs-technik AEG-Telefunken-Handbücher, Band 16*. Berlin, Germany: Elitera-Verlag, 1974.

[14] C. Sourkounis, "Active minimization of cumulated load in the drive train by dynamic speed flexible operation," *Prz. Elektrotech. (Elect. Rev.)*, vol. 85, no. 10, pp. 267–271, 2009.

[15] K. Sugiura and Y. Hori, "Vibration suppression in 2- and 3-mass system based on the feedback of imperfect derivative of the estimated Torsional torque," *IEEE Trans. Ind. Electron.*, vol. 43, no. 1, pp. 56–64, Feb. 1996.

Constantinos Sourkounis (M'06) received the Dipl.-Ing and Dr.-Ing degrees from Clausthal University of Technology (TU Clausthal), Clausthal-Zellerfeld, Germany, in 1989 and 1994, respectively.

After he received the Ph.D. degree, he became the Chief Engineer in the Institute of Electrical Power Engineering at TU Clauthal. In 2003, he received his habilitation. Since 2003, he has been a Professor at Ruhr-University Bochum, Bochum, Germany, heading the Power System Technology Research Group. His main research areas are mechatronic drive systems, renewable energy sources, decentralized energy systems supplied by renewable energy sources, and energy supply systems for transportation systems.